European Polymer Journal 79 (2016) 1–12

Contents lists available at ScienceDirect

European Polymer Journal

journal homepage: www.elsevier.com/locate/europolj

Macromolecular Nanotechnology

Synergic effect of cellulose and lignin nanostructures in PLA based systems for food antibacterial packaging

W. Yang [a], E. Fortunati [a], F. Dominici [a], G. Giovanale [b], A. Mazzaglia [b], G.M. Balestra [b], J.M. Kenny [a], D. Puglia [a,*]

[a] University of Perugia, Civil and Environmental Engineering Department, Materials Engineering Center, UdR INSTM, Terni, Italy
[b] University of Tuscia, Department of Agricultural Sciences and Forestry (DAFNE), Via S. Camillo De Lellis snc, 01100 Viterbo, Italy

ARTICLE INFO

Article history:
Received 6 February 2016
Received in revised form 25 March 2016
Accepted 3 April 2016
Available online 4 April 2016

Keywords:
Poly (lactic acid)
Cellulose nanocrystals
Lignin nanoparticles
Plant pathogens

ABSTRACT

Ternary polymeric films based on poly (lactic acid), obtained dispersing cellulose nanocrystals (CNC) and lignin nanoparticles (LNP) at two different amounts (1 and 3 wt%), respectively in neat PLA and glycidyl methacrylate (GMA) grafted PLA (g-PLA), were produced by melt extrusion. Thermal, optical and mechanical properties, as well as the morphologies of CNC and LNP reinforced PLA nanocomposites, were investigated. Results from UV–Vis characterization have confirmed a synergic effect of LNP and CNC based nanostructures in terms of transparency and UV light blocking capability. In addition, the combination of the two lignocellulosic nanofillers proved to be effective also in nucleation and crystal growth, with increased cristallinity values for ternary systems in comparison with binary nanocomposites. Furthermore, the ternary nanocomposites showed both higher strength and modulus values than those of neat PLA and PLA binary systems. Lignin nanoparticles and cellulose nanocrystals, when combined with neat or grafted poly (lactic acid), have shown antibacterial activity with reduction in multiplication of the bacterial plant pathogen *Pseudomonas syringae* pv. *tomato* (Pst). In particular, results from PLA nanocomposite films containing lignin nanoparticles pointed out how this green functionality allows to develop innovative strategies, towards harmful pathogens, helpful in the food packaging sector.

1. Introduction

Biodegradable plastics offer a promising alternative to petroleum-based plastics. While petroleum-based products use oil in their manufacturing and take up space in landfills, biodegradable plastics can be synthesized in bacteria or plants and have the potential to be disposed of in a way that is less damaging to the environment. Among them, poly (lactic acid) (PLA) is a very promising material, due to its excellent mechanical properties, transparency and commercial availability. However, it has many drawbacks, such as slow degradation rate, brittleness, that make it not suitable for applications demanding mechanical performance, unless suitably modified. Another limitation of PLA towards its wider industrial application is its limited gas barrier property, which prevents its complete access to industrial sectors such as packaging; many research studies have focused on overcoming these limitations [1–3]. In this context, it has been demonstrated that the addition of

* Corresponding author.
E-mail address: debora.puglia@unipg.it (D. Puglia).

http://dx.doi.org/10.1016/j.eurpolymj.2016.04.003
0014-3057/

renewable nanoreinforcements as cellulose nanocrystals (CNC) contributes to increase the barrier to gases due to the different synergic effects of tortuosity, crystal nucleation and chain immobilization [3–11]. Some previous research works have highlighted the significant advantages of using CNC with PLA, including water vapour and oxygen barrier effects, migration level below packaging normative requirements [12] and antimicrobial properties when combined with silver nanoparticles [4,13] or essential oil [14], demonstrating the antimicrobial potential of PLA/CNC films as promising bioactive packaging for the preservation of fresh food products against food borne pathogens.

Lignin, as the second most abundant renewable and biodegradable natural resource next to cellulose [6,8], contains many functional groups in different proportion in its structure, providing scope for chemical modification and adjustment of polarity to produce compatibility with appropriate polymeric matrices [15,16], specific antioxidant properties [17,18] and UV stabilization effect [19–21]. It has been demonstrated that the radical scavenging activity of this renewable filler depends on particle size and it is improved when the filler is used at the nanoscale [22], moreover enhanced thermal and mechanical properties of different polymer matrices, like phenolic foams [23], poly (vinyl alcohol) [24], natural rubber [25] and PLA based materials [26] have been confirmed when lignin nanoparticles (LNP) were incorporated. Another relevant property of lignin is its antibacterial activity: it can be considered as a promising green principle useful against dangerous microorganisms, its inherent biocidal activity allows to reduce the environmental problems related to the use of silver nanoparticles and improves the release of active principles in agriculture [27,28]. This effect has been also studied by Domenek et al. [18], which investigated, in the field of material applications, the antioxidant activity of micro-scaled lignin as a natural substitute of synthetic antioxidants for the protection of the food, opening the access to the realization of active packaging materials compounded with natural antioxidant substances.

In the context of frame of food preservation, few studies have been reported on the use of organic active principles (vegetal) against bacteria/fungi plant pathogens [29–31], while a wide literature is available on how these active agents can be incorporated in biobased polymeric matrices, such as PLA [2]. It has to be reminded how damages and economic losses of agriculture productions caused by plant pathogens, like *Pseudomonas syringae* pv. *tomato* on tomato plant/fruits, represent a serious worldwide problem that needs innovative and green strategies able to preserve important fresh productions during their transport and storage.

Recently, the possibility to obtain various functionalities by using the combination of different nanofillers, including antimicrobial activity, was also considered. Fortunati et al. [12,13,32,4] investigated the combination of CNC with silver nanoparticles in PLA based nanocomposites and they studied how to improve the important industrial problem of slow crystallization of PLA by using CNC as biobased nucleating agents and low antibacterial performance of the neat matrix introducing silver nanoparticles. Looking at the results from recent studies related to the use of cellulose and lignin in ternary formulations, Ago et al. [33] produced defect-free electrospun fibres from aqueous dispersions of lignin, poly (vinyl alcohol) (PVA), and CNC. The results showed that phase separated domains were observed in lignin-rich/PVA solvent casted films. Interestingly, the size of the phase separated domains was reduced by the addition of CNC, but no surface effects were observed with the addition of CNC in PVA-rich fibres. In another study [34], the thermo-mechanical performance of lignin-based electrospun fibres and spin-coated thin films was improved when they were embedded with CNC, as revealed from the results of dynamic mechanical analysis (DMA) and nanoindentation tests (the elastic modulus increased substantially while adding 15 wt% of CNC into lignin/PVA (75:25) films).

However, no examples are reported in the literature on the combination of cellulose nanocrystals and nanoscaled lignin on PLA films and how their synergic combination could affect the final performance even in terms of antimicrobial activity. In this study, CNC and LNP were premixed in different masterbatches based on PLA or modified PLA matrix (glycidyl methacrylate melt grafted PLA), with the aim to produce and characterize high performance PLA based nanocomposites for active food packaging applications. Indeed, both the use of a masterbatch approach (in the case of CNC) and reactive grafting (in the case of LNP), have been confirmed as effective solutions to improve the dispersion of these nanofillers in PLA and enhance the performance of resulted nanocomposites, as reported in our previous studies [26,35]. With the aim of evaluating their possible synergic effects, binary and ternary PLA based nanocomposites containing both CNC and LNP were prepared by combining the two processing procedure (masterbatch and reactive melt grafting). Thermal, optical, and mechanical properties, such as antibacterial activity of the selected films towards a plant/fruit pathogen were tested and here reported.

2. Materials and methods

2.1. Materials

Poly (lactic acid) (PLA 3251D), with a specific gravity of 1.24 g/cm^3, a relative viscosity of ca. 2.5, and a melt flow index (*MFI*) of 35 g/10 min (190 °C, 2.16 kg) was supplied by NatureWorks LLC, USA. Glycidyl methacrylate (GMA), with a density of 1.042 g/mL at 25 °C, and dicumyl peroxide (DCP), with a density of 1.56 g/mL at 25 °C, were supplied by Sigma-Aldrich®. Pristine lignin, obtained as bio-residue of conversion of *Arundo donax* L. biomass to bioethanol in a steam explosion pretreatment, followed by enzymatic reactions and filtration, was supplied by CRB (Centro Ricerca Biomasse, University of Perugia) [36]. Microcrystalline cellulose (MCC, dimensions of 10–15 μm) was supplied by Sigma-Aldrich®.

2.2. Lignin nanoparticle (LNP) and cellulose nanocrystal (CNC) synthesis

LNP suspension was prepared from pristine lignin by hydrochloric acidolysis presented in our previous study [37]. CNC suspension was prepared from MCC by sulphuric acid hydrolysis [12]. Details were also introduced in our previous study [35].

2.3. Preparation of masterbatches (MBs)

GMA grafting was performed in a twin-screw microextruder (DSM Explorer 5&15 CC Micro Compounder) in the presence of DCP as initiator. Screw speed of 100 rpm, mixing time of 8 min and a temperature profile of 165–175–180 °C were selected to realize the grafting reaction [35]. The content of PLA grafted with GMA (g-PLA), to be used as a compatibilizer in the resulted nanocomposites, was fixed at 15 wt% [38]. Different masterbatches were then obtained by mixing various amounts of LNP and CNC, respectively with g-PLA and PLA. Compositions and colour variation of different masterbatches are reported in Fig. 1.

2.4. PLA nanocomposite processing

Binary and ternary nanocomposite films were manufactured by using a twin-screw microextruder as well. Conditions of 100 rpm screw speed, 2 min of dwell time and a kneading temperature of 180–195–210 °C were employed to optimize material final properties, after which, a film forming process with a head force of 180 N and a die temperature of 200 °C was used, in order to obtain PLA and PLA nanocomposite films with mean values of thickness (t) ranging from 20 up to 80 μm. The materials, designed as PLA/3CNC (t = 48 μm) and PLA-3LNP (t = 40 μm) with direct incorporation of 3 wt% of CNC and LNP (mixing time 2 min) after 8 min of PLA heating, were produced as control, while the ternary PLA nanocomposite films having the code PLA-1LNP/1CNC (t = 56 μm) consisted of 85 wt% MB1 and 15 wt% MB3, respectively. The system containing 85 wt% of MB2 and 15 wt% of MB3 was denoted as PLA-1LNP/3CNC (t = 20 μm), while PLA-3LNP/1CNC (t = 64 μm) represented the material composed of 85 wt% of MB1 and 15 wt% of MB4. Finally, PLA-3LNP/3CNC (t = 76 μm) was indicated as the material obtained through the mixture of 85 wt% MB2 and 15 wt% MB4. The final compositions of all the different formulations are also reported in Table 1.

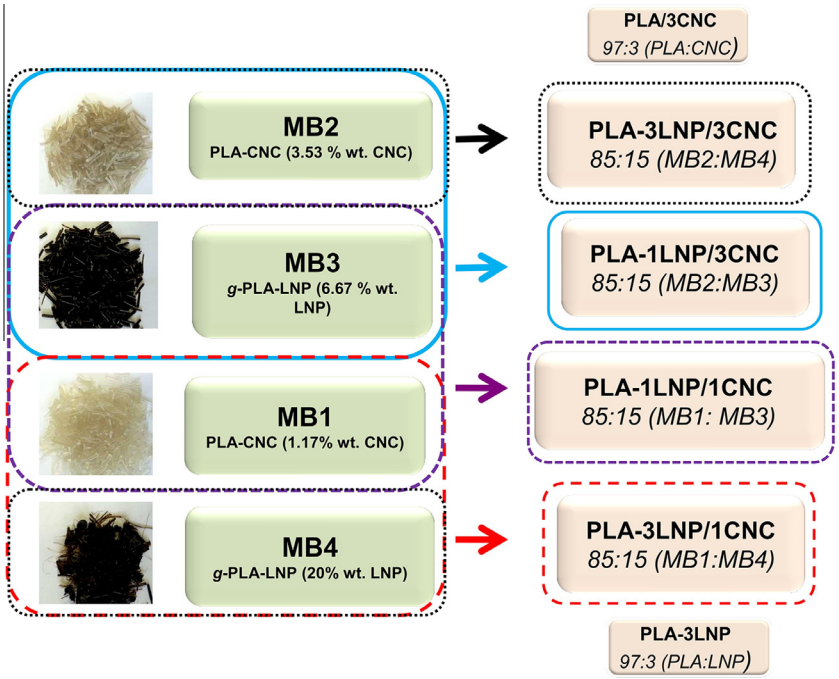

Fig. 1. Definition of masterbatches (visual appearance, material content) and preparation of PLA nanocomposite films containing cellulose nanocrystals and lignin nanoparticles in binary and ternary systems.

Table 1
Nanocomposite formulations.

Formulations	PLA (%)	g-PLA (wt%)	LNP (wt%)	CNC (wt%)
PLA	100	–	–	–
PLA-1LNP/1CNC	83	15	1	1
PLA/3CNC	82	15		3
PLA-1LNP/3CNC	81	15	1	3
PLA/3LNP	82	15	3	–
PLA-3LNP/1CNC	81	15	3	1
PLA-3LNP/3CNC	79	15	3	3

2.5. Optical properties

Light transmittance of the nanocomposites was measured using a Varian (Cary 4000, USA) ultraviolet–visible (UV–Vis) spectrophotometer. The scan was carried out from 250 nm to 1100 nm with a scan speed of 240 nm/min and the transmittance signal was normalized to the actual thickness value of the different films.

2.6. Differential scanning calorimetry (DSC)

DSC (TA Instrument, Q200) measurements were performed in the temperature range from −25 to 210 °C at 10 °C/min under nitrogen flow. PLA and PLA nanocomposite samples (6–8 mg) were heated from −25 to 210 °C at a rate of 10 °C/min and held at 210 °C for 2 min to erase the thermal history (1st scan), then they were cooled to −25 at 10 °C/min and reheated under the same conditions (2nd scan). Glass transition, cold crystallization and melting temperatures (T_g, T_{cc} and T_m) were determined from the first and second heating scans. The cristallinity degree (χ) was calculated from the second scan as:

$$\chi = \frac{\Delta H_m}{\Delta H_{m0}(1 - m_f)} \times 100 \quad (1)$$

where ΔH_m is the enthalpy for melting, ΔH_{m0} is enthalpy of melting for a 100% crystalline PLA sample, taken as 93 J/g [39] and $(1 - m_f)$ is the weight fraction of PLA in the sample.

2.7. Thermogravimetric analysis (TGA)

TGA was carried out using a thermogravimetric analyzer (TGA, Seiko Exstar 6300). The samples, approximately 8 mg, were heated from 30 to 700 °C at a heating rate of 10 °C/min under nitrogen atmosphere. The weight-loss rate was obtained from derivative thermogravimetric (DTG) data. The onset degradation temperature (T_{onset}) was defined as the 1% weight loss drawn from the TG curves after 200 °C at which the samples begin to degrade. Maximum thermal degradation temperature (T_{max}) was also collected from DTG peaks maxima.

2.8. Mechanical behavior

The mechanical performance of neat PLA and PLA nanocomposite systems was evaluated by means of tensile tests, performed on rectangular probes (100 mm × 10 mm) on the basis of UNI ISO 527 standard with a crosshead speed of 5 mm/min, a load cell of 500 N and an initial gauge length of 25 mm. Average tensile strength (σ), Young's modulus (E) and elongation at break (ε_b) were calculated from the resulting stress-strain curves. The measurements were done at room temperature and at least five samples were tested for each material.

2.9. Morphological behavior

The microstructure of PLA and PLA nanocomposite films was investigated by FESEM, by checking the surface morphology of samples fractured in liquid nitrogen and gold sputtered.

2.10. Antibacterial activity

Biocidal activity of neat PLA film and PLA nanocomposites containing lignin nanoparticles and/or cellulose nanocrystals was evaluated against the bacterial plant pathogen *P. syringae* pv. *tomato* (Pst), the causal agent of tomato (*Lycopersicon esculentum* Mill.) bacterial speck. This bacterium affects worldwide tomatoes grown/production causing serious damages on all organs, including fruits that result unmarketable [30]. In particular, the antibacterial activity of the binary and ternary nanocomposites produced with the highest content of LNP nanoparticles (PLA/3LNP and PLA-3LNP/1CNC) was evaluated and tested respect to a known (CFBP 1323) Pst strain, utilized at a concentration of 1×10^6 CFU/mL; PLA neat film was also tested and used as control thesis. Pst strain subculture was obtained by growing bacterium for 48–72 h at 25 ± 2 °C using a

solid Nutrient Agar (NA) supplemented by Sucrose 5% (NAS). The experiments were carried out using Nutrient Broth (NB) 4% by the liquid medium test [40]. The thesis (PLA as control, PLA/3LNP and PLA-3LNP/1CNC) were constituted by 3 replicates each; 5 sterile glass tubes per thesis, each containing 5 mL of liquid broth (NB) with 1×10^6 CFU/mL of Pst and 1 sample (3.24 cm^2) per nanocomposite films, were arranged. All tubes were placed on a reciprocal shaker for 48 h at 25 ± 2 °C at 150 rpm. Samplings from all tubes/thesis were carried out at 0 (h after bacterial inoculation), 3, 12, 24 h and serial dilution were carried out and plated on NAS. After 48 h at 25 ± 2 °C the number of Pst bacterial colonies was counted. All data were statistically elaborated using GraphPad Prism 4 software by analysis of variance (ANOVA) and significance of treatments was determined using Tukey's HSD test ($p \leqslant 0.05$) [41].

3. Results and discussion

3.1. Optical properties

Barrier to UV light is an important property to be considered in the case of polymeric films that have to be used as packaging materials, especially when protection of light-sensitive products during storage is required [42]; even if PLA is widely used as a packaging material, it has poor UV barrier properties that need to be improved in order to expand the application sectors. Results from UV–Vis characterization and related visual aspect of PLA, PLA binary and ternary nanocomposites are reported in Fig. 2a and b and Table 2. Neat PLA showed the highest transmission in the visible region of the spectra (400–700 nm) and UV light region (250–400 nm). No significant changes were observed with CNC incorporation (even at the higher concentration, PLA/3CNC, the films resulted highly transparent). The good transparency of PLA/3CNC films has been related with the good dispersion of CNC into PLA matrix [43]. The colour distribution in the film suggests that CNC nanocrystals were uniformly distributed confirming the good dispersion obtained during the processing of the PLA nanocomposites. On the other hand, LNP showed a good blocking effect in the UV light region in the case of PLA-1LNP/1CNC and PLA-3LNP, as already observed in our previous studies [37]. When the CNC dose increased up to 3 wt% (PLA-1LNP/3CNC), a further decrease of the UV light transmission was observed. This behavior may be attributed to a synergistic effect between LNP and CNC fillers: whereas LNP served as blocking agents of UV light irradiation, CNC seems to behave like mirrors, transmitting part of the UV light source and reflecting it at the same time, and further blocking it when LNP fillers are found [44]. It has been demonstrated that mixing CNC with lignin at an appropriate ratio (even without the use of a polymeric substrate) enabled the formation of optically transparent nanocomposite films that simultaneously displayed high transmittance in the visible spectrum and zero transmittance in the UV spectrum [45]. We have supposed that the same behavior can be considered in the case of polymeric films containing LNP and CNC, confirming that, even in presence of a polymeric matrix, the aromatic lignin polymer could dislocate the π–π aromatic aggregates on the surface of the cellulosic nanoparticles, increasing the extinction coefficient and decreasing the transmittance in the UV region. The schematic diagram was presented in Fig. 3. This behavior was more evident in the case of PLA/3LNP and PLA-3LNP/1CNC, while the lowest UV light transmission was obtained in PLA-3LNP/3CNC film. Results showed that all the ternary nanocomposite films showed a blocking effect in the UV light spectra region, while maintaining the high transparency in the visible spectra region.

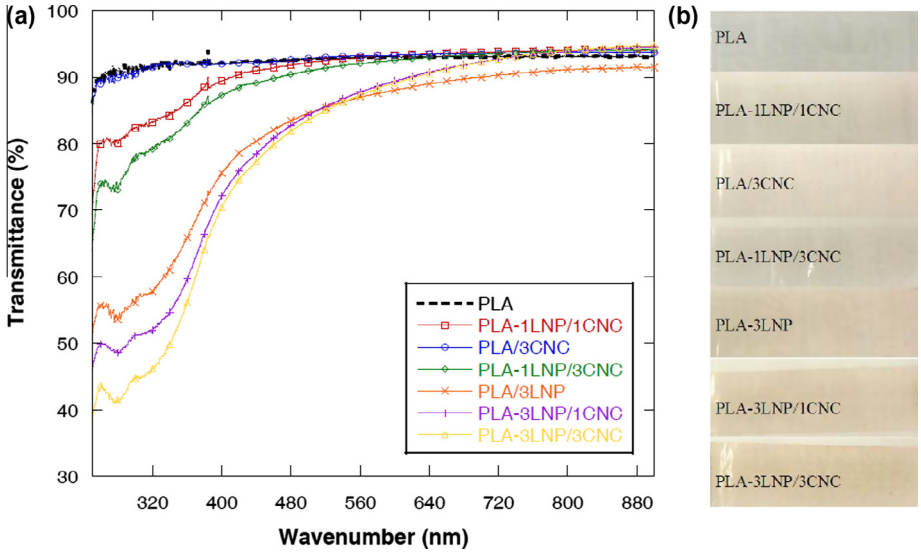

Fig. 2. UV–Vis spectra of PLA and PLA nanocomposite films containing CNC and LNP nanoparticles in binary and ternary systems (a) and visual appearance of the films (b).

Table 2
UV–Vis and TGA results for different films based on PLA containing CNC and LNP.

Formulations	Transmittance (%) at λ = 320 nm	$T_{onset\ (1\%)}$ (°C)	T_{max} (°C)
PLA	91.4	266.1	360.3
PLA-1LNP/1CNC	83.1	283.3	359.8
PLA/3CNC	91.5	255.5	345.5
PLA-1LNP/3CNC	79.1	286.1	360.7
PLA/3LNP	57.8	272.3	341.4
PLA-3LNP/1CNC	51.9	274.3	351.9
PLA-3LNP/3CNC	46.2	262.1	347.1

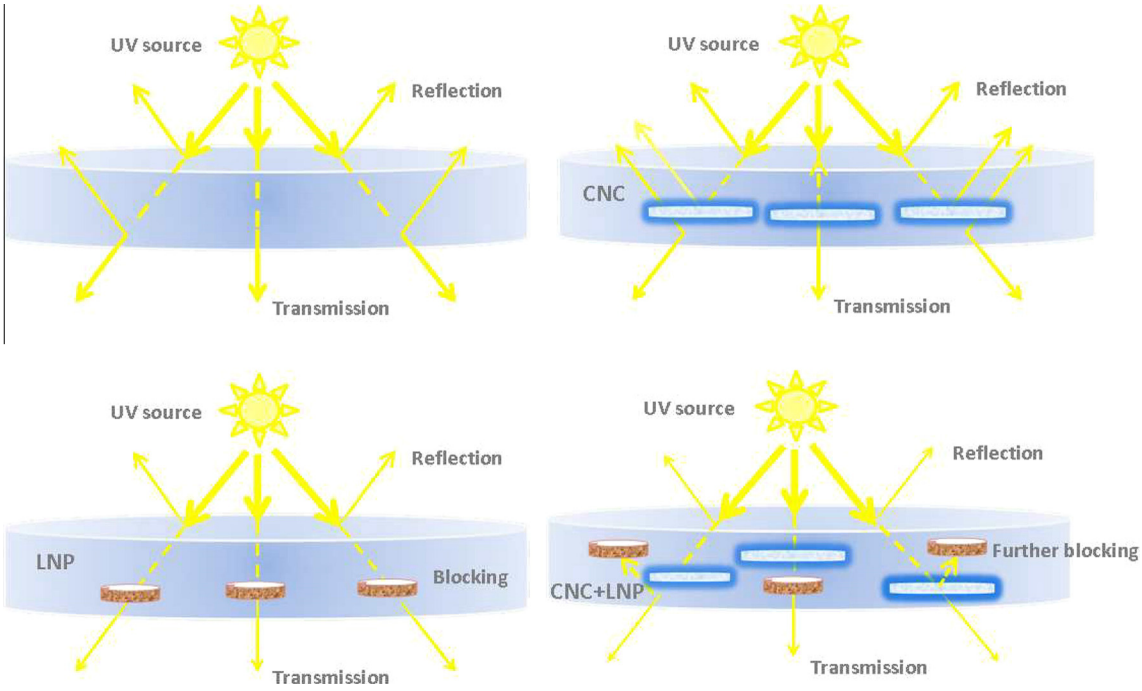

Fig. 3. Synergic effect of LNP and CNC nanoparticles in terms of transparency and UV light blocking capability.

3.2. Thermal properties

DSC analysis was used to investigate the thermal behavior of PLA and PLA nanocomposites containing LNP and CNC (glass transition (T_g), cold crystallization (T_{cc}) and melting temperatures (T_m) were measured); moreover the final cristallinity values of the selected systems were evaluated. The curves of first heating (Fig. 4a), cooling (Fig. 4b) and second heating scan (Fig. 4c) were reported, while all the calorimetric parameters were evaluated and summarized in Table 3. The measured T_g and T_m temperatures do not differ significantly from that of neat PLA (61.1 ± 0.1 and 169.1 ± 0.8 °C), and a similar tendency was also observed in the second heating scan. It was also observed that the recrystallization capability increased for PLA nanocomposites, with a reduction in T_{cc} in comparison with neat PLA (104.0 ± 0.5 °C). The presence of GMA grafted on PLA matrix, combined with the use of a masterbatch approach, promoted the dispersion of LNP and CNC, representing an important factor on the different crystallization behavior of the resulted nanocomposites [35,46]. In the cooling scan shown in Fig. 4b, exothermic peaks with low intensity were observed for the pure PLA, indicating a rather low crystallization capability. In the other cases of PLA samples filled with LNP or CNC, especially PLA-3LNP/3CNC, the crystallization peaks had relatively higher intensity and started from higher temperature as a result of enhanced tendency to crystallize. The nucleation effect was remarkably enhanced when homogeneous nanostructure dispersion in PLA and good interaction with the matrix were achieved [47]. During the second heating scan, different levels of decreased T_{cc} of binary and ternary PLA nanocomposites were detected, with respect to neat PLA: specifically PLA-3LNP/3CNC presented the lowest T_{cc} valued (96.3 ± 0.1 °C) (Table 3). The cristallinity degree (χ), calculated from the second scan, was also reported. It has been previously discussed that the incorporation of LNP or CNC would enhance the PLA crystallization ability [12,35,47]. Slight higher cristallinity

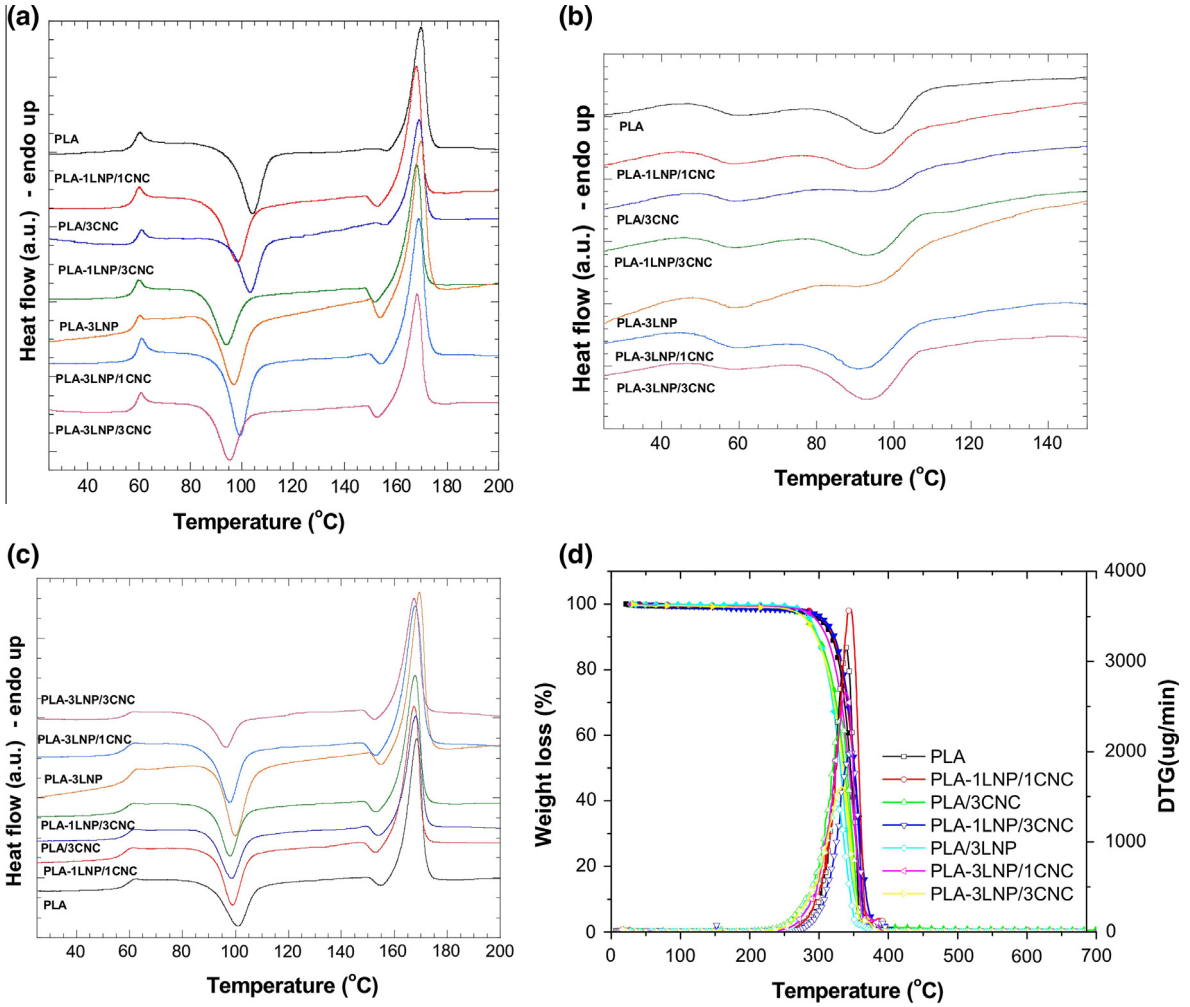

Fig. 4. DSC thermograms related to the (a) first heating scan, (b) cooling scan and (c) second heating scan; residual mass curves and derivative curves vs temperature (d) of PLA and PLA nanocomposite films containing cellulose nanocrystals and lignin nanoparticles in binary and ternary systems.

Table 3
Thermal parameters (T_g, T_{cc}, T_m) of PLA and PLA nanocomposites (1st and 2nd heating scan).

Formulations	First heating scan			Second heating scan			
	T_g (°C)	T_{cc} (°C)	T_m (°C)	T_g (°C)	T_{cc} (°C)	T_m (°C)	X_c (%)
PLA	60.1 ± 0.1	104.0 ± 0.5	169.1 ± 0.8	59.1 ± 0.7	100.6 ± 0.6	167.8 ± 0.6	18.0 ± 1.3
PLA-1LNP/1CNC	60.1 ± 0.1	98.6 ± 0.1	168.2 ± 0.3	58.5 ± 0.6	98.9 ± 0.2	167.4 ± 0.1	23.1 ± 0.3
PLA/3CNC	60.8 ± 0.1	103.0 ± 0.1	169.0 ± 0.1	59.6 ± 0.7	97.8 ± 0.7	167.8 ± 0.3	22.4 ± 2.3
PLA-1LNP/3CNC	59.7 ± 0.1	94.1 ± 0.1	167.9 ± 0.1	58.3 ± 0.1	97.8 ± 0.3	167.6 ± 0.1	23.6 ± 0.6
PLA/3LNP	60.3 ± 0.03	96.1 ± 0.7	169.3 ± 0.2	59.8 ± 0.5	99.7 ± 0.2	168.8 ± 0.4	20.6 ± 2.6
PLA-3LNP/1CNC	61.1 ± 0.01	99.4 ± 0.4	168.9 ± 0.1	59.1 ± 0.7	97.9 ± 0.1	167.8 ± 0.1	23.2 ± 0.9
PLA-3LNP/3CNC	60.6 ± 0.01	95.3 ± 0.3	168.0 ± 0.1	59.0 ± 0.2	96.3 ± 0.1	167.3 ± 0.1	32.2 ± 0.1

values were observed in PLA-1LNP/1CNC (23.1 ± 0.3%) in comparison with PLA/3CNC (22.4 ± 2.3%) and PLA/3LNP (20.6 ± 2.6%), confirming that the combination of g-PLA with masterbatch procedures could favour the nucleation effect and the crystal growth. It can be supposed that the LNP and CNC have a synergistic effect also on nucleation and crystal growth, since ternary nanocomposite (PLA-1LNP/1CNC), even at the lower nanofiller content, showed higher cristallinity degree (23.1 ± 0.3) than binary nanocomposites (PLA/3CNC and PLA/3LNP), while a substantial improvement was detected in PLA-3LNP/3CNC (32.2 ± 0.1%).

3.3. Thermogravimetric analysis

TG and DTG curves of neat PLA and PLA based binary and ternary nanocomposites are shown in Fig. 4d. Thermal parameters including T_{onset}, and T_{max} were summarized in Table 2. T_{onset} of neat PLA was 266.1 °C, while was 255.5 °C for PLA/3CNC, indicating that the addition of 3 wt%. CNC did not improve the heat resistance of resulted nanocomposite films, due to the inferior interfacial adhesion between CNC and PLA matrix, and easiness of aggregation for pristine cellulose nanocrystals [12,13,47]. However, interestingly, the incorporation of 3 wt% LNP into PLA showed an opposite result, since a T_{onset} of 272.3 °C was observed. This behavior could be probably attributed to the homogeneous dispersion of lignin nanoparticles and enhanced interactions between PLA matrix and LNP. The different thermal behavior should be ascribed to the difference in chemical structures of CNC and LNP. When using the masterbatch procedures and GMA as compatibilizer, a remarkable increase of T_{onset} was obtained with respect to neat PLA or binary system nanocomposites, as the T_{onset} of PLA-1LNP/1CNC was measured as 283.3 °C. Multiple effects (masterbatch effect, compatibilization effect and probable synergistic effect of CNC and LNP) could prominently improve the thermal properties of nanocomposites. A further increase of temperature for onset degradation was detected when increasing the CNC loading up to 3 wt% (T_{onset} of PLA-1LNP/3CNC was 286.1 °C). In the meanwhile, the T_{onset} of PLA-3LNP/1CNC (274.3 °C) was also slightly improved when compared with PLA/3LNP. However, when the content of nanofillers rise up to 6 wt% (PLA-3LNP/3CNC), a detrimental effect occur (T_{onset} = 262.1 °C), even lower than that of neat PLA. This result could be due to the possible presence of agglomerations at such high loading of LNP and CNC. For the T_{max}, a similar tendency as T_{onset} could be seen. It should be noted that the introduction of LNP or CNC does not increase the T_{max}, and this may due to the same range of degradation temperature of LNP or CNC with respect to PLA, as reported in our previous study [37]. Overall, the film PLA-1LNP/3CNC exhibited the optimal heat resistance behavior in the studied bionanocomposites.

3.4. Mechanical properties

Fig. 5(a–c) show the results of tensile test in terms of strength (σ), modulus (E), and elongation at break (ε_b), while the typical stress-strain curves for all the studied formulations are reported in Fig. 5d. Values of PLA/3LNP binary nanocomposite are also reported for comparison. All studied nanocomposites showed higher tensile strength and Young's modulus mean values than neat PLA except PLA/3LNP, with higher values detected for the ternary PLA-1LNP/3CNC nanocomposite. In the case of PLA/3LNP, the observed reduction of σ and E, along with the increase of ε_b, may be justified considering the formation of crazes in the deformation process, that could initiate between LNP and PLA and further developing into mature crazes to absorb more energy. LNP did not only served as nucleation agents, but also acted as toughening agents to increase the ductility of PLA matrix, as already observed in our previous study [26]. Consequently, the PLA/3LNP nanocomposites exhibited remarkable improvements in toughness compared with neat PLA. Similar behaviors were also detected by some other authors [48,49]. In the ternary systems, we have observed that the same total amount of different nanofillers (4 wt%) showed different behaviors: PLA-1LNP/3CNC system exhibited higher values of modulus and tensile strength than those of PLA-3LNP/1CNC, showing a more obvious enhancement effect for cellulose nanocrystals than lignin nanoparticles. The different effects of LNP and CNC in PLA matrix may be attributed to the different interactions due to different chemical structures between them, since more functional groups (carbonyl, phenolic or aliphatic hydroxyls, carboxyl, etc.) can be found in different proportions of lignin with respect to the single polysaccharide structure of CNC. When the content of nanofillers increased to 6 wt% (PLA-3LNP/3CNC), a limited reinforcement effect was observed, due to the formation of aggregates. Furthermore, the ternary system nanocomposites also showed higher strength and modulus than those of neat PLA and binary system nanocomposites. These results highlight the different effects of reinforcement exerted by CNC and LNP, and the efficiency of the selected compatibilizer in the structure of studied nanocomposite systems. The different mechanical behaviors of binary and ternary nanocomposites will expand the application range in the packaging industry sector.

3.5. Morphological behavior

FESEM micrographs of neat PLA and PLA nanocomposite fractured surfaces are presented in Fig. 6. A smooth fractured surface could be seen in neat PLA and PLA/3LNP, suggesting a good interface adhesion between LNP and PLA matrix. No micro-domains can be observed, the surface resulted homogeneous due to a good dispersion of LNP nanofillers in PLA matrix during the process, confirming the observed mechanical performance of the nanocomposites containing lignin nanoparticles at the selected weight amount (3 wt%). Furthermore, the nanocomposite film loaded with CNC (PLA/3CNC) showed a rougher fractured surface in comparison with neat PLA, evidencing a more brittle tendency of this formulation. When CNC and LNP are combined at the different weight content, it is clearly visible how higher amount of lignin (PLA-3LNP/1CNC and PLA-3LNP/3CNC) maintained the surface homogeneity in comparison with PLA-1LNP/1CNC and PLA-1LNP/3CNC samples. The morphological results are consistent with tensile tests (Fig. 5).

3.6. Antibacterial activity

Results of antibacterial tests for PLA and PLA nanocomposites films are reported in Fig. 7. We have observed that neat PLA film reveals its inability to contrast the bacterial cell multiplication over the time, since it seems to support a Pst growth with

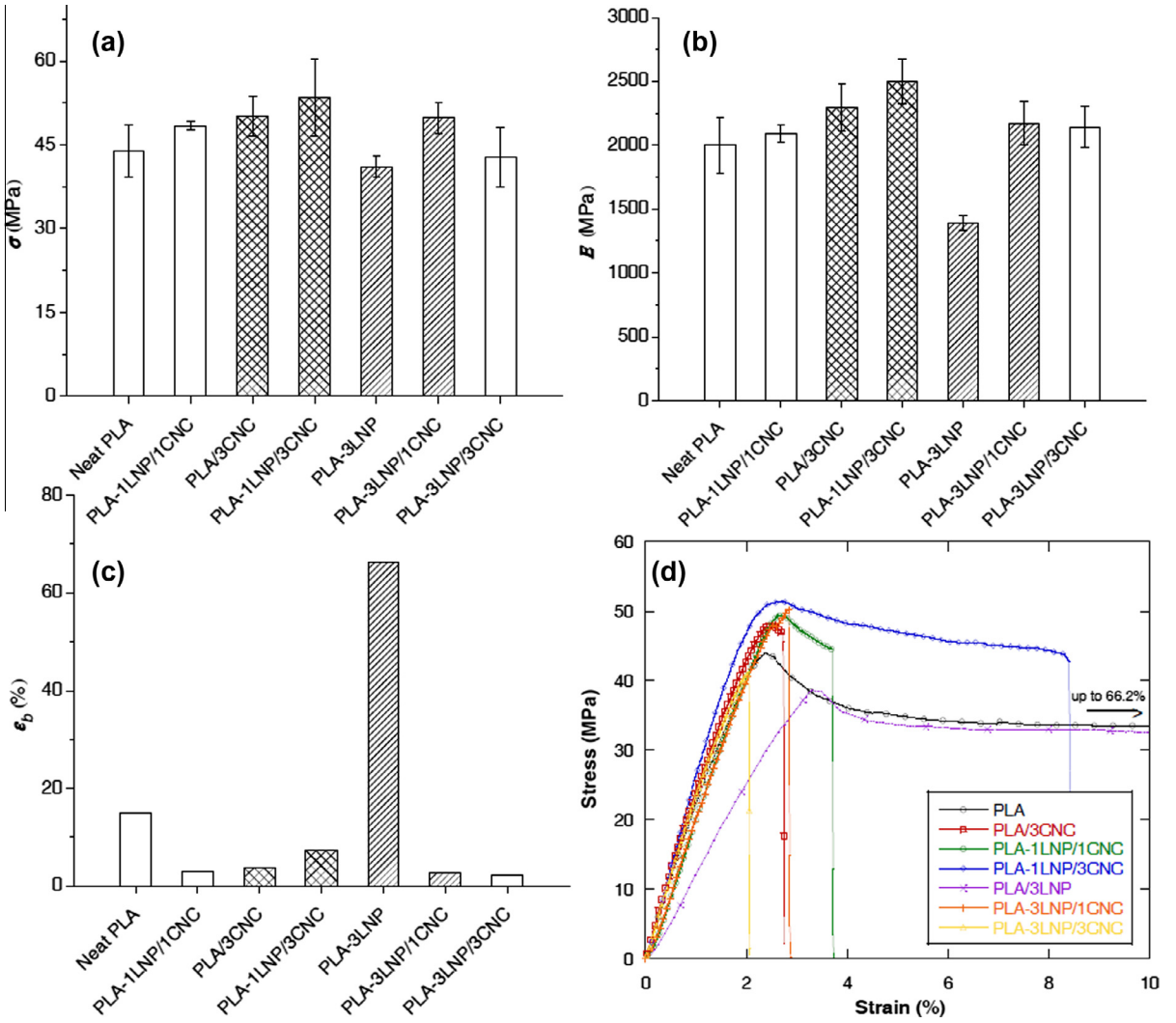

Fig. 5. Values for tensile strength (a), Young's modulus (b), elongation at break (c) and stress-strain curves of PLA and PLA nanocomposite films containing cellulose nanocrystals and lignin nanoparticles in binary and ternary systems.

bacterial values that increased from 1×10^6 to 8.4×10^7 CFU/mL in 24 h. On the other hand, an antibacterial activity of PLA matrix against Pst was monitored in presence of lignin nanoparticles and cellulose nanocrystals. In the case of PLA-3LNP/1CNC based nanocomposite, the antibacterial activity was much more evident respect to PLA control just after few hours (0–3 h) of Pst inoculation. Moreover, the highest antibacterial activity, prolonged over the time, was detected for PLA/3LNP binary formulation. The results from antibacterial test showed the effectiveness of the used lignocellulosic natural sources in the reduction of Pst population multiplication when embedded in a biodegradable polymer matrix, even inoculating the bacteria at a high concentration (1×10^6 CFU/mL). Moreover, the results underlined the more evident antimicrobial effect exerted by lignin nanoparticles: the antibacterial activity of lignin is usually related to its origin, and specifically due to the presence of phenolic compounds and different functional groups containing oxygen (—OH, —CO, —COOH) in its structure. Furthermore, it is known that its biocidal activity is expressed on bacterial cell membrane causing severe damages and lysis of bacterial cells with consequent release of cell content [50,51]. In our case, the effect of LNP is particularly evident for the PLA/3LNP system, while this effect was mitigated by the presence of CNC. As already observed in DSC characterization, increased cristallinity values of PLA films observed when 1 wt% (PLA-3LNP/1CNC, 23.2%) and 3 wt% (PLA-3LNP/3CNC, 32%) of CNC are incorporated in PLA/3LNP can reduce the diffusion mechanisms and, consequently, the antimicrobial response of the PLA-3LNP/1CNC ternary nanocomposite respect to the LNP based binary film.

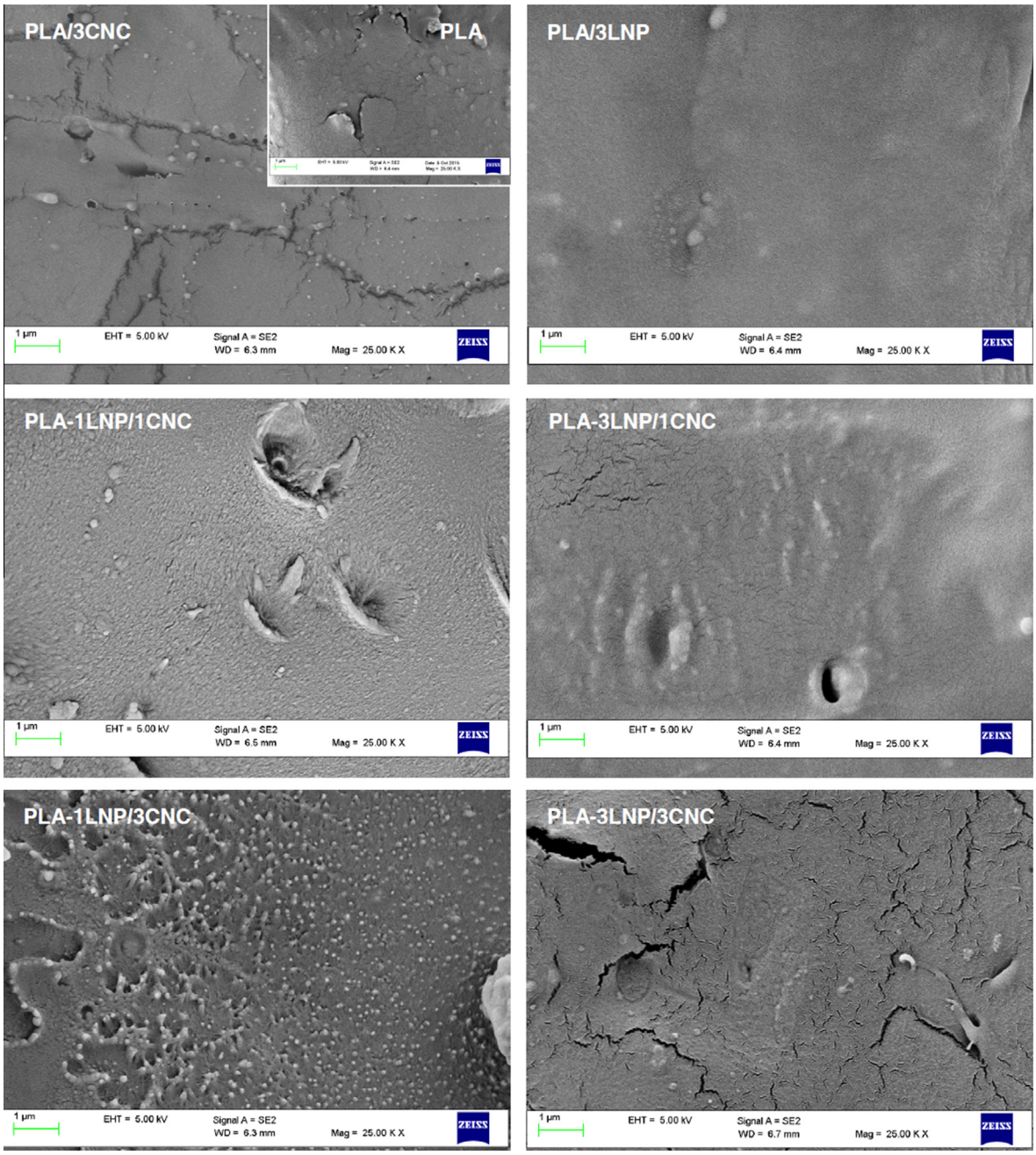

Fig. 6. FESEM images of fractured cross sections for PLA and PLA nanocomposite films containing cellulose nanocrystals and lignin particles in binary and ternary systems.

4. Conclusions

Melt extruded PLA nanocomposite films, obtained by dispersing cellulose nanocrystals (CNC) and lignin nanoparticles (LNP) at two different amounts (1 and 3 wt%), respectively in neat PLA and glycidyl methacrylate (GMA) grafted PLA (g-PLA), were successfully produced and then characterized. The optical characterization of the films confirmed a synergic effect of LNP and CNC nanoparticles in terms of transparency and UV light blocking capability, moreover the combination of the two lignocellulosic nanofillers at the two selected weight content proved to be effective also in enhancing nucleation and crystal growth with respect of binary reference systems (PLA/3LNP and PLA/3CNC). Furthermore, the best mechanical performance, both in terms of tensile strength and elastic modulus, was revealed for the ternary system containing 1 wt% LNP

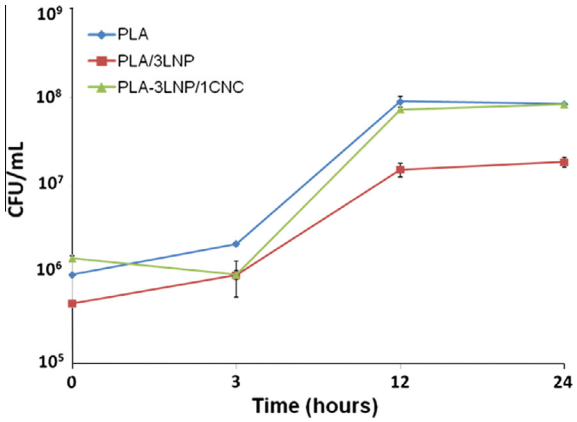

Fig. 7. Antibacterial activity of different films based on neat PLA, PLA film with 3 wt% of lignin nanoparticles (PLA-3LNP), PLA ternary system containing both cellulose nanocrystals (1 wt%) and lignin nanoparticles (3 wt%) (PLA-3LNP/1CNC), on the multiplication of tomato plant pathogenic bacteria *Pseudomonas syringae* pv. *tomato* (Pst) (CFBP 1323) 1×10^6 CFU/mL. The vertical bars represent the standard error of the mean log-transformed Pst populations sizes at given sampling time. Data submitted to the analysis of variance (ANOVA) resulted significant ($p \leqslant 0.05$).

and 3 wt% CNC, confirming the role of cellulose nanostructures in reinforcing PLA based nanocomposites and the real possibility to improve this property adding nanoscaled lignin in a synergic manner. Thermal results, as well as the different obtained morphologies for CNC and LNP reinforced PLA nanocomposites, confirmed that good dispersion of the nanostructures, due to the masterbatch/grafting combination, was achieved. Lastly, the biocidal activity of PLA films (containing lignin nanoparticles and cellulose nanocrystals) against a tomato bacterial plant pathogen was tested and the results confirmed how damages and losses caused by plant pathogens on fresh food in the packaging industry can be monitored by using new and green research lines related to unexplored functionalities of lignin and cellulose structures at the nanoscale.

Acknowledgements

This research has been developed in the frame of the BIT3G Project – Third generation biorefinery integrated in the territory, funded by the Ministry of Education, Universities and Research (Italy) (MIUR-project: CTN01_00063_49295). W.Y. appreciates the funding support of China Scholarship Council (CSC).

References

[1] M. Jamshidian, E.A. Tehrany, M. Imran, M.J. Akhtar, F. Cleymand, S. Desobry, Structural, mechanical and barrier properties of active PLA–antioxidant films, J. Food Eng. 110 (3) (2012) 380–389.
[2] M. Jamshidian, E.A. Tehrany, M. Imran, M. Jacquot, S. Desobry, Poly-lactic acid: production, applications, nanocomposites, and release studies, Compr. Rev. Food Sci. Food Safe. 9 (2010) 552–571.
[3] M. Jonoobi, J. Harun, A.P. Mathew, K. Oksman, Mechanical properties of cellulose nanofiber (CNF) reinforced polylactic acid (PLA) prepared by twin screw extrusion, Compos. Sci. Technol. 70 (12) (2010) 1742–1747.
[4] E. Fortunati, S. Rinaldi, M. Peltzer, N. Bloise, L. Visai, I. Armentano, A. Jiménez, L. Latterini, J.M. Kenny, Nano-biocomposite films with modified cellulose nanocrystals and synthesized silver nanoparticles, Carbohyd. Polym. 101 (30) (2014) 1122–1133.
[5] V.P. Martino, R.A. Ruseckaite, A. Jiménez, L. Averous, Correlation between composition, structure and properties of poly(lactic acid)/polyadipate-based nano-biocomposites, Macromol. Mater. Eng. 295 (2010) 551–558.
[6] Q. Shi, C. Zhou, Y. Yue, W. Guo, Y. Wu, Q. Wu, Mechanical properties and in vitro degradation of electrospun bio-nanocomposite mats from PLA and cellulose nanocrystals, Carbohyd. Polym. 90 (1) (2012) 301–308.
[7] N. Bitinis, E. Fortunati, R. Verdejo, J. Bras, J.M. Kenny, L. Torre, M.A. López-Manchado, Poly (lactic acid)/natural rubber/cellulose nanocrystal bionanocomposites. Part II: Properties evaluation, Carbohyd. Polym. 96 (2) (2013) 621–627.
[8] M.R. Kamal, V. Khoshkava, Effect of cellulose nanocrystals (CNC) on rheological and mechanical properties and crystallization behavior of PLA/CNC nanocomposites, Carbohyd. Polym. 123 (2015) 105–114.
[9] M. Pracella, M.M.-U. Haque, D. Puglia, Morphology and properties tuning of PLA/cellulose nanocrystals bio-nanocomposites by means of reactive functionalization and blending with PVAc, Polymer 55 (16) (2014) 3720–3728.
[10] N. Lin, J. Huang, P.R. Chang, J. Feng, J. Yu, Surface acetylation of cellulose nanocrystal and its reinforcing function in poly(lactic acid), Carbohyd. Polym. 83 (4) (2011) 1834–1842.
[11] A. Iwatake, M. Nogi, H. Yano, Cellulose nanofiber-reinforced polylactic acid, Compos. Sci. Technol. 68 (9) (2008) 2103–2106.
[12] E. Fortunati, I. Armentano, Q. Zhou, D. Puglia, A. Terenzi, L.A. Berglund, J.M. Kenny, Microstructure and nonisothermal cold crystallization of PLA composites based on silver nanoparticles and nanocrystalline cellulose, Polym. Degrad. Stabil. 97 (10) (2012) 2027–2036.
[13] E. Fortunati, I. Armentano, Q. Zhou, A. Iannoni, E. Saino, L. Visai, L.A. Berglund, J.M. Kenny, Multifunctional bionanocomposite films of poly (lactic acid), cellulose nanocrystals and silver nanoparticles, Carbohyd. Polym. 87 (2) (2012) 1596–1605.
[14] S. Salmieri, F. Islam, R.A. Khan, F.M. Hossain, H.M.M. Ibrahim, C. Miao, W.Y. Hamad, M. Lacroix, Antimicrobial nanocomposite films made of poly(lactic acid)–cellulose nanocrystals (PLA–CNC) in food applications—Part B: Effect of oregano essential oil release on the inactivation of Listeria monocytogenes in mixed vegetables, Cellulose 21 (2014) 4271–4285.
[15] P. Frigerio, Biopolymers in Elastomers: Lignins as Biofiller for Tyre Compound, Università degli Studi di Milano-Bicocca, 2014.
[16] K. Bahl, T. Miyoshi, S.C. Jana, Hybrid fillers of lignin and carbon black for lowering of viscoelastic loss in rubber compounds, Polymer 55 (16) (2014) 3825–3835.

[17] C. Pouteau, P. Dole, B. Cathala, L. Averous, N. Boquillon, Antioxidant properties of lignin in polypropylene, Polym. Degrad. Stabil. 81 (1) (2003) 9–18.
[18] S. Domenek, A. Louaifi, A. Guinault, S. Baumberger, Potential of lignins as antioxidant additive in active biodegradable packaging materials, J. Polym. Environ. 21 (3) (2013) 692–701.
[19] N. Smolarski, High-value Opportunities for Lignin: Unlocking Its Potential, Frost & Sullivan, Paris, 2012, pp. 1–15.
[20] Y.-L. Chung, J.V. Olsson, R.J. Li, C.W. Frank, R.M. Waymouth, S.L. Billington, E.S. Sattely, Renewable lignin–lactide copolymer and application in biobased composites, ACS Sustain. Chem. Eng. 1 (10) (2013) 1231–1238.
[21] K. Toh, S. Nakano, H. Yokoyama, K. Ebe, K. Gotoh, H. Noda, Anti-deterioration effect of lignin as an ultraviolet absorbent in polypropylene and polyethylene, Polym. J. 37 (8) (2005) 633–635.
[22] Y. Ge, Q. Wei, Z. Li, Preparation and evaluation of the free radical scavenging activities of nanoscale lignin biomaterials, BioResources 9 (4) (2014) 6699–6706.
[23] B. Del Saz-Orozco, M. Oliet, M.V. Alonso, E. Rojo, F. Rodríguez, Formulation optimization of unreinforced and lignin nanoparticle-reinforced phenolic foams using an analysis of variance approach, Compos. Sci. Technol. 72 (6) (2012) 667–674.
[24] S.S. Nair, S. Sharma, Y. Pu, Q. Sun, S. Pan, J.Y. Zhu, Y. Deng, A.J. Ragauskas, High shear homogenization of lignin to nanolignin and thermal stability of nanolignin-polyvinyl alcohol blends, ChemSusChem 7 (2014) 3513–3520.
[25] C. Jiang, H. He, H. Jiang, L. Ma, D.M. Jia, Nano-lignin filled natural rubber composites: preparation and characterization, Express Polym. Lett. 7 (5) (2013) 480–493.
[26] W. Yang, F. Dominici, E. Fortunati, J.M. Kenny, D. Puglia, Effect of lignin nanoparticles and masterbatch procedures on the final properties of glycidyl methacrylate-g-poly(lactic acid) films before and after accelerated UV weathering, Ind. Crops Prod. 77 (2015) 833–844.
[27] A.P. Richter, J.S. Brown, B. Bharti, A. Wang, S. Gangwal, K. Houck, E.A. Cohen Hubal, V.N. Paunov, S.D. Stoyanov, O.D. Velev, An environmentally benign antimicrobial nanoparticle based on a silver-infused lignin core, Nature Biotechnol. 10 (2015) 817–823.
[28] M. Norgren, H. Edlund, Lignin: recent advances and emerging applications, Current Opin. Colloid. Interface Sci. 19 (5) (2014) 409–416.
[29] M.E.I. Badawy, S.A.M. Abdelgaleil, Composition and antimicrobial activity of essential oils isolated from Egyptian plants against plant pathogenic bacteria and fungi, Ind. Crops Prod. 52 (2014) 776–782.
[30] A. Quattrucci, E. Ovidi, A. Tiezzi, V. Vinciguerra, G.M. Balestra, Biological control of tomato bacterial speck using Punica granatum fruit peel extract, Crop Prot. 46 (2013) 18–22.
[31] G.M. Balestra, A. Heydari, D. Ceccarelli, E. Ovidi, A. Quattrucci, Antibacterial effect of *Allium sativum* and *Ficus carica* extracts on tomato bacterial pathogens, Crop Prot. 28 (2009) 807–811.
[32] E. Fortunati, M. Peltzer, I. Armentano, A. Jiménez, J.M. Kenny, Combined effects of cellulose nanocrystals and silver nanoparticles on the barrier and migration properties of PLA nano-biocomposites, J. Food Eng. 118 (1) (2013) 117–124.
[33] M. Ago, J.E. Jakes, L.-S. Johansson, S. Park, O.J. Rojas, Interfacial properties of lignin-based electrospun nanofibers and films reinforced with cellulose nanocrystals, ACS App. Mater. Interfaces 4 (12) (2012) 6849–6856.
[34] M. Ago, J.E. Jakes, O.J. Rojas, Thermomechanical properties of lignin-based electrospun nanofibers and films reinforced with cellulose nanocrystals: a dynamic mechanical and nanoindentation study, ACS Appl. Mater. Interfaces 5 (22) (2013) 11768–11776.
[35] W. Yang, F. Dominici, E. Fortunati, J.M. Kenny, D. Puglia, Melt free radical grafting of glycidyl methacrylate (GMA) onto fully biodegradable poly (lactic) acid films: effect of cellulose nanocrystals and a masterbatch process, RSC Adv. 5 (41) (2015) 32350–32357.
[36] F. Cotana, G. Cavalaglio, A. Nicolini, M. Gelosia, V. Coccia, A. Petrozzi, L. Brinchi, Lignin as co-product of second generation bioethanol production from ligno-cellulosic biomass, Energy Procedia 45 (2014) 52–60.
[37] W. Yang, J.M. Kenny, D. Puglia, Structure and properties of biodegradable wheat gluten biocomposites containing lignin nanoparticles, Ind. Crops Prod. 74 (2015) 348–356.
[38] J. Liu, H. Jiang, L. Chen, Grafting of glycidyl methacrylate onto poly(lactide) and properties of PLA/starch blends compatibilized by the grafted copolymer, J. Polym. Environ. 20 (2012) 810–816.
[39] O. Martin, L. Avérous, Poly(lactic acid): plasticization and properties of biodegradable multiphase systems, Polymer 42 (14) (2001) 6209–6219.
[40] N.W. Schaad, J.B. Jones, W. Chun, Laboratory Guide for Identification of Plant Pathogenic Bacteria, third ed., APS Press, St. Paul, MN, USA, 2001.
[41] R.G. Steel, J.H. Torrie, D.A. Dickey, Principles and procedures of statistics: A biometrical approach, 3 sub edition., McGraw-Hill Series in Probability and Statistics, McGraw-Hill Companies, 1996.
[42] R. Auras, B. Harte, S. Selke, An overview of polylactides as packaging materials, Macromol. Biosci. 4 (9) (2004) 835–864.
[43] M.P. Arrieta, E. Fortunati, F. Dominici, E. Rayón, J. López, J.M. Kenny, PLA-PHB/cellulose based films: mechanical, barrier and disintegration properties, Polym. Degrad. Stabil. 107 (2014) 139–149.
[44] A. Hambardzumyan, L. Foulon, B. Chabbert, V. Aguie-Beghin, Natural organic UV-absorbent coatings based on cellulose and lignin: designed effects on spectroscopic properties, Biomacromolecules 13 (2012) 4081–4088.
[45] A. Hambardzumyana, M. Molinari, N. Dumelie, L. Foulon, A. Habrant, B. Chabbert, V. Aguié-Béghin, Structure and optical properties of plant cell wall bio-inspired materials: cellulose–lignin multilayer nanocomposites, C.R. Biol. 334 (11) (2011) 839–850.
[46] D. Wu, L. Wu, L. Wu, B. Xu, Y. Zhang, M. Zhang, Nonisothermal cold crystallization behavior and kinetics of polylactide/clay nanocomposites, J. Polym. Sci. B Polym. Phys. 45 (2007) 1100–1113.
[47] A. Pei, Q. Zhou, L.A. Berglund, Functionalized cellulose nanocrystals as biobased nucleation agents in poly(l-lactide) (PLLA) – crystallization and mechanical property effects, Compos. Sci. Technol. 70 (5) (2010) 815–821.
[48] Y. Sun, L. Yang, X. Luc, C. He, Biodegradable and renewable poly (lactide)–lignin composites: synthesis, interface and toughening mechanism, J. Mater. Chem. A 3 (2015) 3699–3709.
[49] O. Gordobil, I. Egüés, R. Llano-Ponte, J. Labidi, Physicochemical properties of PLA lignin blends, Polym. Degrad. Stabil. 108 (2014) 330–338.
[50] J. Zemek, B. Kosikova, J. Augistin, D. Joniak, Antibiotic properties of lignin components, Folia Microbiol. 24 (1979) 483–486.
[51] G. Cazacu, M. Capranu, V.I. Popa, Advances concerning lignin utilization in new materials, in: S. Thomas, P.M. Visakh, A.P. Mathew (Eds.), Advances in Natural Polymers, vol. 18, 2012, pp. 278–308.